Stability and Multiattractor Dynamics of a Toggle Switch Based on a Two-Stage Model of Stochastic Gene Expression

Michael Strasser,[†] Fabian J. Theis,[†‡] and Carsten Marr[†*]
[†]Institute for Bioinformatics and Systems Biology, Helmholtz Zentrum München, German Research Center for Environmental Health, Neuherberg, Germany; and [‡]Institute for Mathematical Sciences, Technische Universität München, Garching, Germany

ABSTRACT A toggle switch consists of two genes that mutually repress each other. This regulatory motif is active during cell differentiation and is thought to act as a memory device, being able to choose and maintain cell fate decisions. Commonly, this switch has been modeled in a deterministic framework where transcription and translation are lumped together. In this description, bistability occurs for transcription factor cooperativity, whereas autoactivation leads to a tristable system with an additional undecided state. In this contribution, we study the stability and dynamics of a two-stage gene expression switch within a probabilistic framework inspired by the properties of the Pu/Gata toggle switch in myeloid progenitor cells. We focus on low mRNA numbers, high protein abundance, and monomeric transcription-factor binding. Contrary to the expectation from a deterministic description, this switch shows complex multiattractor dynamics without autoactivation and cooperativity. Most importantly, the four attractors of the system, which only emerge in a probabilistic two-stage description, can be identified with committed and primed states in cell differentiation. To begin, we study the dynamics of the system and infer the mechanisms that move the system between attractors using both the quasipotential and the probability flux of the system. Next, we show that the residence times of the system in one of the committed attractors are geometrically distributed. We derive an analytical expression for the parameter of the geometric distribution, therefore completely describing the statistics of the switching process and elucidate the influence of the system parameters on the residence time. Moreover, we find that the mean residence time increases linearly with the mean protein level. This scaling also holds for a one-stage scenario and for autoactivation. Finally, we study the implications of this distribution for the stability of a switch and discuss the influence of the stability on a specific cell differentiation mechanism. Our model explains lineage priming and proposes the need of either high protein numbers or long-term modifications such as chromatin remodeling to achieve stable cell fate decisions. Notably, we present a system with high protein abundance that nevertheless requires a probabilistic description to exhibit multistability, complex switching dynamics, and lineage priming.

INTRODUCTION

During differentiation, a cell and its progeny cascade through a number of lineage decisions from stem cells over progenitor cells to mature functional cells. Many decisions are assumed to be binary and realized by a toggle switch, a simple cellular memory device. This network module consists of two genes, inhibiting each other via mutual promoter binding. In each differentiating cell, one gene will eventually win this biomolecular battle, inhibiting the other gene and subsequently activating its lineage-determining downstream targets. In hematopoiesis, the generation of blood cells, a series of gene switches has been found to determine the differentiation path of hematopoietic stem cells and to direct the ratio of mature blood cells (1,2). The most prominent example in this context is the mutual inhibition of Gata-1 and Pu.1, two transcription factors responsible for the development of erythroid and myeloid blood cells from common myeloid progenitors (3–5).

Due to its importance in development, toggle switches are subject to both experimental and theoretical investigations (for a review, see Macarthur et al. (6)). Using a deterministic framework under the assumption of large molecule numbers, Cherry and Adler (7) discussed criteria for working switches. More specifically Roeder and Glauche (8), Huang et al. (9), and Chickarmane et al. (10) used a simple deterministic model of the toggle switch based on ordinary differential equations to describe the Pu.1–Gata-1 switch in hematopoiesis. A comprehensive overview and comparison of the different deterministic toggle switch models is provided by Duff et al. (11).

All these studies focus on the steady states of the switch and the parameter dependent bifurcations in a deterministic framework. However, protein variations of a differentiating cell influence the dynamics of the decision-making process and lead to stochastic transitions between the two steady states. This randomness is induced by gene expression noise, which has been shown to be ubiquitous in biological systems due to low molecule numbers (12). Thus, the probabilistic frameworks, developed to account for gene expression noise (see Paulsson (13) for a review), have to be applied to understand fundamental aspects of toggle switch properties.

Probabilistic models of the toggle switch account for low copy numbers and intrinsic fluctuations. In Kepler and Elston (14), the dynamics of an exclusive switch, where

Submitted June 6, 2011, and accepted for publication November 22, 2011.

*Correspondence: carsten.marr@helmholtz-muenchen.de

Carsten Marr's present address is Centre for Systems Biology at Edinburgh, University of Edinburgh, Edinburgh, UK.

Editor: Andre Levchenko.

0006-3495/12/01/0019/11 $2.00

doi: 10.1016/j.bpj.2011.11.4000

two genes share the same promoter, is discussed within a probabilistic framework. A comparison of simple switch circuitries is given in Warren and ten Wolde (15). Contrary to deterministic models, transitions between the two macroscopic regimes where one of the two genes dominates are possible due to the inherently noisy gene transcription (16,17), even without cooperative binding of transcription factors (18). More recent contributions focused on analytic descriptions (19,20), the switching time between macroscopic regimes for different regulatory realizations (16,21,22) or parameter regimes (17), boundaries for the switching time (23), or delay effects (24). Notably, all of these approaches are based on a one-stage model of gene expression, where DNA is directly processed into functional proteins. However, it has been shown that the characteristics of protein noise strongly depend on the underlying expression model (25,26).

In this contribution, we abstract the regulatory details of the prominent myeloid Pu.1-Gata-1 mutual inhibition. Contrary to common belief, which advocates the lumping of the two stages of expression, we show that the inclusion of both mRNA and protein leads to an interesting change in system dynamics. The probabilistic two-stage description exhibits complex multiattractor dynamics without autoactivation and cooperativity. Remarkably, a 2006 study reported low numbers of mRNAs in single murine blood cells: Warren et al. (27) found ~10 transcripts per cell of the murine PU.1 gene in common myeloid progenitors. Based on these findings we study a probabilistic description of a toggle switch with low mRNA numbers, high protein abundance, and (in accordance with the known role of Pu.1) monomeric transcription factor binding. We deliberately choose the simplest toggle switch model and neglect autoactivation due to our ignorance of the logic of activation and inhibition at the promoter. However, our results can easily be extended and are discussed for the case of dimeric regulation and exclusive autoactivation.

RESULTS

A toggle switch based on a two-stage model of gene expression

We describe the mutual inhibition of two genes, further on called A and B, using a two-stage model of gene expression (25,26) with mutual inhibition being realized as DNA-protein binding (see Fig. 1). This kind of switch has been implemented in vivo by Gardner et al. (28). The model can be represented as a set of biochemical reactions for A and B, respectively, and a set of reaction rates α, β, etc.:

$$\begin{aligned} \mathrm{DNA_A} &\xrightarrow{\alpha_A} \mathrm{DNA_A} + \mathrm{mRNA_A}, \\ \mathrm{DNA_B} &\xrightarrow{\alpha_B} \mathrm{DNA_B} + \mathrm{mRNA_B}, \end{aligned} \tag{1}$$

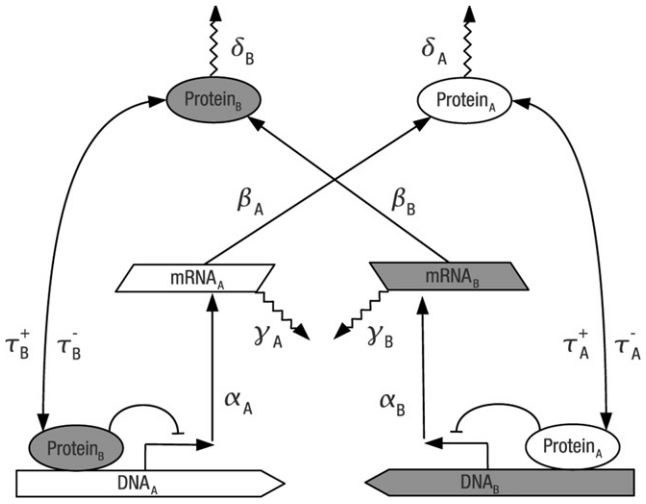

FIGURE 1 Scheme of the two-stage switch. (*Open*) Species associated with gene A; (*shaded*) species associated with gene B. (*Solid arrows*) Synthesis and binding. (*Jagged arrows*) Degradation. $\mathrm{mRNA_A}$ is transcribed from $\mathrm{DNA_A}$ with rate α_A. It decays with rate γ_A and is translated into $\mathrm{Protein_A}$ with rate β_A. $\mathrm{Protein_A}$ decays with rate δ_A and can bind (unbind) $\mathrm{DNA_B}$ with rate $\tau_A^+(\tau_A^-)$. Protein-bound DNA leads to transcriptional arrest. The topology is symmetric with respect to the genes A and B, thus, the same reactions exist for B.

$$\begin{aligned} \mathrm{mRNA_A} &\xrightarrow{\gamma_A} \varnothing, \\ \mathrm{mRNA_B} &\xrightarrow{\gamma_B} \varnothing, \end{aligned} \tag{2}$$

$$\begin{aligned} \mathrm{mRNA_A} &\xrightarrow{\beta_A} \mathrm{mRNA_A} + \mathrm{Protein_A}, \\ \mathrm{mRNA_B} &\xrightarrow{\beta_B} \mathrm{mRNA_B} + \mathrm{Protein_B}, \end{aligned} \tag{3}$$

$$\begin{aligned} \mathrm{Protein_A} &\xrightarrow{\delta_A} \varnothing, \\ \mathrm{Protein_B} &\xrightarrow{\delta_B} \varnothing, \end{aligned} \tag{4}$$

$$\begin{aligned} \mathrm{Protein_A} + \mathrm{DNA_B} &\xrightarrow{\tau_A^+} \mathrm{DNA_B^{bound}}, \\ \mathrm{Protein_B} + \mathrm{DNA_A} &\xrightarrow{\tau_B^+} \mathrm{DNA_A^{bound}}, \end{aligned} \tag{5}$$

$$\begin{aligned} \mathrm{DNA_B^{bound}} &\xrightarrow{\tau_A^-} \mathrm{Protein_A} + \mathrm{DNA_B}, \\ \mathrm{DNA_A^{bound}} &\xrightarrow{\tau_B^-} \mathrm{Protein_B} + \mathrm{DNA_A}. \end{aligned} \tag{6}$$

Reactions 1 and 2 correspond to mRNA transcription from an unbound promoter and mRNA degradation, respectively. Reactions 3 and 4 resemble protein translation and degradation. Reactions 5 and 6 describe the binding and unbinding of a protein to the antagonistic gene and thereby the transition from an active to an inactive promoter and vice versa. Bound DNA lacks the ability to be transcribed. We emphasize that here τ^+ and τ^- are rates rather than times. Note that we assume monomeric transcription factor binding as the simplest of regulatory interaction (which has recently been

shown to be able to induce bimodal gene expression (18)). Our system's topology is symmetric with regard to the two genes, and so are Reactions 1–6, upon the exchange of gene labels A and B.

This model of gene expression is a highly simplified abstraction of the complex processes in the cell. Condensing transcription into a single biochemical reaction does not account for the various steps required to transcribe a gene, e.g., the assembly of the transcription initiation complex, unwinding of DNA or transition of the polymerase to elongation phase. Postprocessing and transport mechanisms are also neglected. However, simplified models of gene expression have successfully been applied to experimental data, supporting the validity of these simplifications (9,30,31).

Most commonly one will study the properties of the system in a deterministic framework using ordinary differential equations (ODEs) that describe the time-evolution of species concentrations (7–10). The ODEs can directly be inferred from Reactions 1–6 assuming mass action kinetics,

$$\begin{aligned}\frac{d}{dt}d_{\mathrm{A}} &= \tau_{\mathrm{B}}^{-}(1-d_{\mathrm{A}}) - \tau_{\mathrm{B}}^{+}d_{\mathrm{A}}n_{\mathrm{B}},\\ \frac{d}{dt}d_{\mathrm{B}} &= \tau_{\mathrm{A}}^{-}(1-d_{\mathrm{B}}) - \tau_{\mathrm{A}}^{+}d_{\mathrm{B}}n_{\mathrm{A}},\end{aligned} \tag{7}$$

$$\begin{aligned}\frac{d}{dt}m_{\mathrm{A}} &= \alpha_{\mathrm{A}}d_{\mathrm{A}} - \gamma_{\mathrm{A}}m_{\mathrm{A}},\\ \frac{d}{dt}m_{\mathrm{B}} &= \alpha_{\mathrm{B}}d_{\mathrm{B}} - \gamma_{\mathrm{B}}m_{\mathrm{B}},\end{aligned} \tag{8}$$

$$\begin{aligned}\frac{d}{dt}n_{\mathrm{A}} &= \beta_{\mathrm{A}}m_{\mathrm{A}} - \delta_{\mathrm{A}}n_{\mathrm{A}} + \tau_{\mathrm{A}}^{-}(1-d_{\mathrm{B}}) - \tau_{\mathrm{A}}^{+}d_{\mathrm{B}}n_{\mathrm{A}},\\ \frac{d}{dt}n_{\mathrm{B}} &= \beta_{\mathrm{B}}m_{\mathrm{B}} - \delta_{\mathrm{B}}n_{\mathrm{B}} + \tau_{\mathrm{B}}^{-}(1-d_{\mathrm{A}}) - \tau_{\mathrm{B}}^{+}d_{\mathrm{A}}n_{\mathrm{B}},\end{aligned} \tag{9}$$

where d_* is the abundance of unbound DNA$_*$, m_* is the abundance of mRNA$_*$ and n_* is the abundance of Protein$_*$ for $*\in\{\mathrm{A},\mathrm{B}\}$.

Bound DNA is expressed in terms of unbound DNA due to mass conservation. Solving Eqs. 7–9 at steady state by setting all time derivatives to zero yields two solutions, one being biologically irrelevant due to its negative species abundances. Given nonnegative initial conditions, the system will always converge toward the positive steady-state solution (32), given by (see the Supporting Material for details)

$$m_{\mathrm{A}}^{(ss)} = m_{\mathrm{B}}^{(ss)} = -\frac{\delta\tau^{-}}{2\beta\tau^{+}}(1-\eta), \tag{10}$$

$$n_{\mathrm{A}}^{(ss)} = n_{\mathrm{B}}^{(ss)} = -\frac{\tau^{-}}{2\tau^{+}}(1-\eta), \tag{11}$$

$$d_{\mathrm{A}}^{(ss)} = d_{\mathrm{B}}^{(ss)} = \frac{2}{1+\eta}, \tag{12}$$

with

$$\eta = \sqrt{\frac{4\alpha\beta\tau^{+}}{\gamma\delta\tau^{-}} + 1}.$$

All parameters are positive and for simplicity assumed to be symmetric for players A and B ($\alpha = \alpha_{\mathrm{A}} = \alpha_{\mathrm{B}},\ldots$).

We now assess the stability of the positive solution Eqs. 10–12 using standard linear stability analysis. To reduce the complexity of our system for the stability analysis, we apply a quasi-steady-state approximation to the DNA binding/dissociation process ($\dot{d}_{\mathrm{A}} = \dot{d}_{\mathrm{B}} = 0$), reducing the dimensionality of our system to four equations. We evaluate the corresponding Jacobian at the single positive solution and use the Hurwitz criterion to verify that all its eigenvalues have negative real part. We conclude that the system has one stable positive fixed point but we cannot analytically exclude the existence of limit cycles. However, inspection of the systems phase portrait (see Fig. S4 in the Supporting Material) indicates that no limit cycles exist. Summarizing, we showed that the deterministic model has only one steady-state solution and is thus monostable.

However, because the deterministic approach is only valid in the limit of large numbers, small molecule numbers of DNA, mRNA, and possibly proteins advocate a discrete probabilistic description of the toggle switch. We define the state of the system at time t as a vector $x(t)$, where $x_i(t) \in \mathbb{N}_0$ is the abundance of species i at time t. Note that the state space is discrete as opposed to the deterministic model. To emphasize this difference we use the uppercase notation D_{A}, D_{B}, M_{A}, M_{B}, N_{A}, and N_{B} for the number of molecules of the respective species. We can describe how the probability $\mathcal{P}(x,t)$ of being in a certain state x changes over time by using the master equation of the system (33)

$$\dot{\mathcal{P}}(x,t) = \sum_{x'}\left[w_{xx'}\mathcal{P}(x',t) - w_{x'x}\mathcal{P}(x,t)\right].$$

The first term considers transitions from states x' with rate $w_{xx'}$ to state x, whereas the second term accounts for transitions from x to all other possible states x' with transition rates $w_{x'x}$. The transition rates, also called propensities (34), are determined by the reaction rates and the number of reagents of the corresponding reactions (see Section S2 in the Supporting Material for an explicit form of the master equation of the system).

Even though the master equation describes the dynamics of the system more accurately than ODEs (most obviously for low particle numbers), it is still an approximation of cellular dynamics as it assumes spatial homogeneity inside a cell and does not account for time delays. Still, the protein distribution predicted by the master equation of a two-stage expression model was indeed observed experimentally (35), supporting the stochastic two-stage model.

Because the master equation for the switch is analytically solvable only for a number of approximations (see, e.g., Walczak et al. (36)) and not integrable for large molecule abundances, we simulate the system trajectories using Gillespie's algorithm (37). Each trajectory follows the master equation, and the set of infinite trajectories constitutes the distribution that solves the master equation. To obtain appropriate parameter values for stochastic simulations, we delineate upper bounds for synthesis parameters from biophysical arguments and adapt degradation parameters to fit desired molecular levels. Table S1 in the Supporting Material lists all used parameter values. Additionally, the analysis below has been conducted for a second, differently motivated set of parameters (see Fig. S3), and yields qualitatively identical results.

Dynamics and quasipotential

In this section we discuss the main features of the switch dynamics. Contrary to the deterministic model, time courses of the stochastic toggle switch model show multistable behavior (Fig. 2 *A*). Given the parameters in Table S1, our toggle switch can adopt different attractors: The two attractors where one player dominates the other (called S_A and S_B depending on which player dominates) are clearly visible in Fig. 2 *A*. A careful inspection of the timecourse and the probability distribution in Fig. 2 *A* shows that there also exist two intermediate attractors where protein numbers are similar ($N_A - N_B \approx 0$). These attractors are called S^*_A and S^*_B from now on. In the timecourses of the system (Fig. 2 *A*) one observes that the system frequently switches between the dominating and the intermediate attractors.

To get a deeper understanding of the complex dynamics of the system, the notion of a quasipotential can be used. The quasipotential U of the system is calculated through the relation $U(x) = -\log \mathcal{P}^{(ss)}(x)$, where $\mathcal{P}^{(ss)}(x)$ is the steady-state distribution of the system. The number of dimensions of the state space where the quasipotential is defined equals the number of species in the system. Here the probability $\mathcal{P}^{(ss)}(x)$ of a state x in steady state is estimated from 15,000 stochastic simulation runs obtained by the StochKit software toolkit (38). In Fig. 2 *B*, the projection of the quasipotential on the N_A–N_B, M_A–M_B plane is shown. The four attractors S_A, S_B, S^*_A, and S^*_B can be seen clearly in the quasipotential of the system. The two attractors S_A and S_B appear as basins at the lower-left and upper-right corners of Fig. 2, whereas the intermediate attractors S^*_A and S^*_B are located at the center, and are not well separated. The dominating attractors can easily be distinguished from the intermediate attractors via parameter-dependent thresholds χ_A, χ_B in the protein dimension (see Section S4 in the Supporting Material).

Importantly, one has to keep in mind that the system considered is out of equilibrium and that the dynamics of a nonequilibrium system are not entirely determined by the gradient of the quasipotential but by an additional curl flux stemming from the nonintegrability of the system (39). As a consequence, barrier heights in the quasipotential do not necessarily correlate with the probability of crossing the barrier.

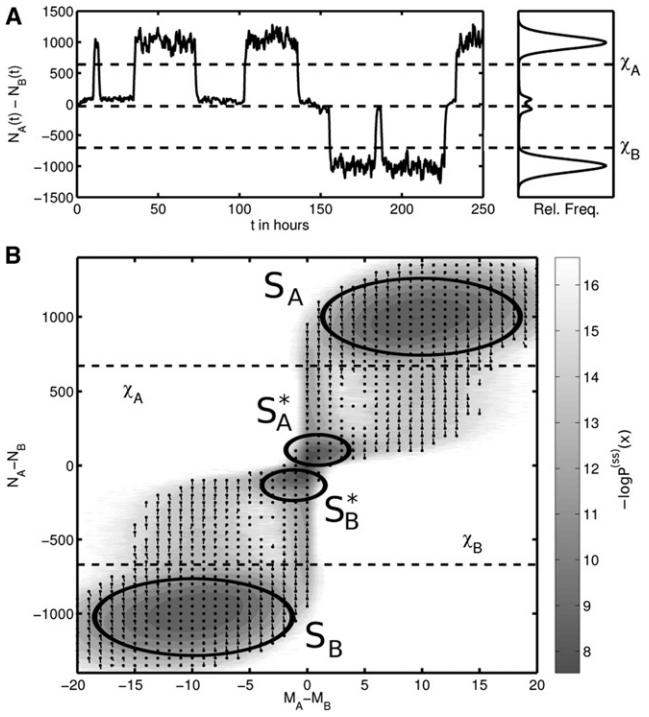

FIGURE 2 Dynamics and quasipotential of the switch showing the different attractors of the system. (*A*) The timecourse of $N_A(t) - N_B(t)$ clearly shows the dominating attractors, which can be separated in state space via the thresholds χ_A and χ_B. Either A dominates (attractor S_A), or B dominates (attractor S_B), or the system is temporarily locked by two bound promoters with only marginal protein expression of A or B (attractors S^*_A and S^*_B). A histogram of $N_A(t) - N_B(t)$ is shown on the right. (*B*) The quasipotential, defined as $U(x) = -\log P^{(ss)}(x)$, includes the mRNA dimension of the system. It shows the four possible attractors as basins in a probability landscape. S_A and S_B are visible as basins at the lower-left and upper-right corners, whereas S^*_A and S^*_B are located around the origin ($N_A - N_B = M_A - M_B = 0$) of the landscape. The outflux $F(x)$ acting on the system at the state x is depicted as a line with a solid circle representing the origin of the vector $F(x)$. Note that the outflux is different from the concept of deterministic field lines. These vectors show that there are different paths for entering and leaving the dominating attractors. Parameters for the simulation are given in Table S1 in the Supporting Material.

To understand the dynamics of the switch in more detail, we therefore consider, for each state x in the state space, the outflux $F(x)$ acting on the system at this point (16). We calculate the outflux as

$$F(x) = \mathcal{P}^{(ss)}(x) \sum_y \mathcal{P}(y|x)(y - x),$$

where the probability $\mathcal{P}(y|x)$ of state y succeeding state x and the probability $\mathcal{P}^{(ss)}(x)$ are calculated from stochastic simulations. Note that the outflux is different from the concept of field lines used in phase portraits of ordinary

differential equations. The outflux $F(x)$ is plotted as small arrows in Fig. 2 (vectors are normalized and *circles* correspond to the origin of the vectors) for all states x with $\mathcal{P}^{(ss)}(x) > 2.5 \cdot 10^{-7}$. This indicates where the system will move from the current state on average. Due to this outflux, the system enters and leaves the attractors S_A and S_B through different paths. This phenomenon has been described in Wang et al. (40) and linked to the emergence of time directionality in nonequilibrium systems. To move from high (S_A or S_B) to low protein numbers, the corresponding mRNA number first has to drop. Moving from low to high protein numbers requires the rise of mRNA numbers first.

A different view on the system's dynamics is provided by the quasipotential landscape and outflux in the ${N_A}^{total}$, ${N_B}^{total}$ plane (Fig. 3), where ${N_A}^{total} = (1 - D_B) + N_A$ is the total number of $Protein_A$ in the system, bound to DNA (first term) or free (second term). Choosing ${N_A}^{total}$ and ${N_B}^{total}$ as projected dimensions shows four distinct basins in the quasipotential landscape. Two basins correspond to the attractors S_A and S_B. These are characterized by high amounts of the dominating protein and zero proteins of the repressed species. The attractors S^*_A and S^*_B are now clearly separated. In these two basins a single protein of one species is present and only a moderate protein number of the other species. In the following, we show why these basins emerge and how the system moves between the attractors.

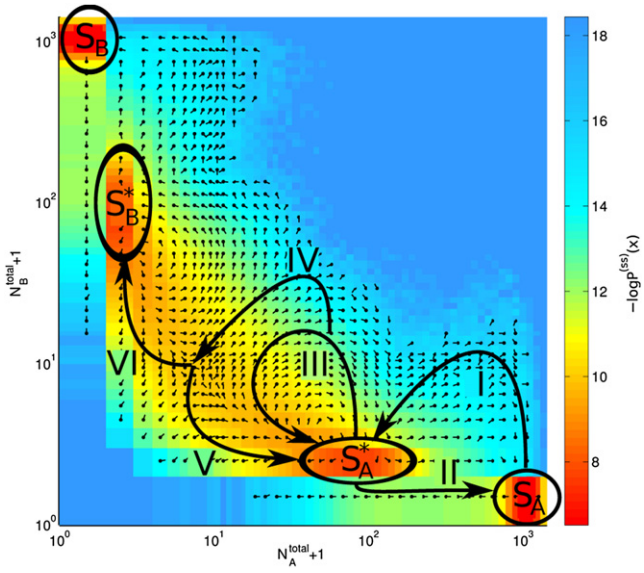

FIGURE 3 Quasipotential of the system projected onto the ${N_A}^{total}$ and ${N_B}^{total}$ dimensions. Note that both axes are on logarithmic scale and are shifted by 1 to include ${N_A}^{total} = 0$ and ${N_B}^{total} = 0$. Therefore, the lowest row in the plot corresponds to the case ${N_B}^{total} = 0$. The quasipotential $U(x) = -\log \mathcal{P}^{(ss)}(x)$ is color-coded (color online: *red areas* reflect minima of the landscape). Visible are four minima corresponding to S_A (*lower right*), S_B (*upper left*), S^*_A (*lower middle*), and S^*_B (*middle left*). The outflux $F(x)$ acting on the system at the state x is depicted as a line with a solid circle representing the origin of the vector $F(x)$. Note that the outflux is different from the concept of deterministic field lines. In contrast to Fig. 2 the vectors are normalized and therefore show only the direction, not the magnitude of the outflux (*Bold arrows*) Typical trajectories (*I–VI*) of the system. For a discussion, see the main text.

We explain the dynamics of the system with a typical trajectory of the system: Let us start with the trajectory in the attractor S_A (*lower right*) where $Protein_A$ dominates $Protein_B$. Due to stochastic fluctuations in the promoter status, eventually a burst of proteins of B will occur and inhibit the promoter of A, whose protein numbers will drop (Fig. 3, trajectory *I*). While the formerly dominating $Protein_A$s are degraded, the newly created $Protein_B$ also quickly decreases in numbers and only one bound $Protein_B$ is saved from degradation. This drives the system toward the origin in the quasipotential of Fig. 3. However, a single $Protein_B$ cannot completely suppress the promoter of DNA_A, leading to a small but constant synthesis of $Protein_A$. The system settles into an intermediate state (S^*_A) defined by the presence of one $Protein_B$ and an intermediate amount of $Protein_A$ originating from the leaky inhibition of DNA_A and bursting.

To leave this basin, the system has one of two options. Either the single $Protein_B$ is degraded when it momentarily is not bound to the promoter. Consequently, the levels of $Protein_A$ rise again and the system reaches S_A. The system is moved to the lower border of the quasipotential where a strong outflux pushes it toward S_A (Fig. 3, trajectory *II*). Alternatively, a burst of $Protein_B$ displaces the system from S^*_A into regions where the vector field points strongly toward the diagonal ${N_A}^{total} = {N_B}^{total}$ (Fig. 3, trajectory *III*). However this burst is typically not strong enough to move the system onto the diagonal and it will fall back into the basin S^*_A. To enable a change from S^*_A to S^*_B, the system has to reach the diagonal. This is accomplished if, while the system is moving toward the diagonal after the burst, additional bursts of $Protein_B$ move it onto the diagonal (Fig. 3, trajectory *IV*). Once the system has hit the diagonal both protein levels will drop to very low numbers because none of the players has any significant advantage. Here by chance the system will move to any side of the diagonal and either toward S^*_A or S^*_B (Fig. 3, trajectories *V* and *VI*).

We find that leaving S^*_A toward S_A (Fig. 3, trajectory *II*) is much more probable than hitting the diagonal from S^*_A (Fig. 3, trajectory *IV*), which would provide the chance of switching. This is obvious from the mechanism described above: Even though the events triggering the two alternatives (degradation of $Protein_B$ and an initial burst of $Protein_B$) have similar probabilities, the diagonal crossing requires additional events and is therefore much less probable. This cannot be deduced from the quasipotential landscape alone: From Fig. 3 it can visually be inferred that the barrier separating S_A and S^*_A is higher than the barrier separating S^*_A and S^*_B. This wrongly suggests that moving between S^*_A and S^*_B occurs more frequently than moving between S_A and S^*_A.

Comparing the system dynamics of our switch with other descriptions we find that i), deterministic one-stage and two-stage models show no bistability, whereas ii), a probabilistic one-stage model exhibits tristability with only one intermediate attractor (see Fig. S2 and Lipshtat et al. (18)). We speculate that translational bursting destabilizes the intermediate attractor of the one-stage model, where neither of the two players can overwhelm the other. Bursting provides an easy mechanism to escape this deadlock situation: It gives whichever player bursts first, a huge advantage over the other, giving rise not only to one protein (as in the one-stage model) but several proteins. As a result, the two-stage system is always quickly pushed away from the diagonal and stabilizes in the attractors S^*_A or S^*_B. Thus, only the combination of a probabilistic description with a two-stage model of gene expression leads to the complex multiattractor dynamics described above.

Residence times

Genetic toggle switches are thought to be involved in the differentiation process of cells. A common idea is that different cell fates correspond to the different attractors of the system (41). Therefore, it is of interest how long the system will stay in one of these attractors. In this contribution, we focus on the time the system will stay in the attractors S_A or S_B. We assume that only in these two attractors is the concentration of either player sufficiently high to carry out a downstream biological function that resembles the switch's decision.

In previous contributions, such quantities have been calculated or determined by stochastic simulation for simpler switch models and were called spontaneous switching time (23), switch lifetime (15), mean first-passage time (14), or switching time (22). Because the switch may flip from a dominating to an intermediate attractor, we choose residence time as the appropriate term for the quantity calculated below. In the following, we derive an analytical approximation for the time the switch stays in a dominating attractor, S_A or S_B, called the residence time t_s. A simulation study for S^*_A/S^*_B suggests qualitatively similar behavior (see Fig. S5).

Let us assume that the system is in attractor S_A. Hence, the promoter of DNA_B is bound by $Protein_A$ whereas the promoter of DNA_A is unbound. We assume that the protein levels in this attractor can be described with the simple two-stage model (25), resulting in a mean $Protein_A$ level of $\overline{N}_A = (\alpha_A\beta_A)/(\gamma_A\delta_A)$. Consequently, the level of $Protein_B$ is $N_B = 0$ as it is inhibited by the high levels of $Protein_A$. To leave S_A, it is crucial that one $Protein_B$ is synthesized, which then can bind the promoter of DNA_A and shut down the synthesis of $Protein_A$, ultimately driving the system out of S_A and into S^*_A. This trajectory (called trajectory *I* in Fig. 3) involves the following events: i), unbinding of $Protein_A$ from DNA_B; ii), synthesis of $Protein_B$ during the unbound phase; and iii), binding of $Protein_B$ to the promoter of DNA_A before $Protein_B$ is degraded.

First, we describe the unbinding of $Protein_A$ from DNA_B. While the system is in S_A, $Protein_A$ dissociates various times, leaving the promoter of DNA_B unbound. The average time the promoter remains unbound, t_u, is equal to the average time until a binding reaction occurs, which is

$$t_u = \frac{1}{\tau^+_A \cdot \overline{N}_A}.$$

The time the promoter stays unbound is a random variable itself, but for simplicity we approximate it with its mean value. Note that t_u depends, somewhat counterintuitively, on τ^+ and not on τ^-, with $\tau^+_A\overline{N}_A$ being the propensity for a binding reaction. Again we emphasize that τ^+ and τ^- are rates (rather than times).

To ultimately synthesize a $Protein_B$, at least one $mRNA_B$ has to be transcribed during t_u and translated before degradation. The probability of k transcription reactions to happen during t_u is

$$P_{\text{Poisson}}(K = k) = \frac{(\alpha_B \cdot t_u)^k}{k!} \cdot \exp(-\alpha_B \cdot t_u),$$

as the number of transcription reactions K during t_u is Poisson-distributed with mean $\alpha_B \cdot t_u$. Thus, the probability of at least one transcription during the unbound phase is

$$q_s = 1 - P(K = 0) = 1 - \exp\left(-\frac{\alpha_B}{\tau^+_A \cdot \overline{N}_A}\right).$$

The probability of translation during an average mRNA lifetime $1/\gamma_B$ is accordingly $q_t = 1 - \exp(-\beta_B/\gamma_B)$. Finally the probability for a binding reaction during average protein lifetime $1/\delta_B$ is $q_b = 1 - \exp(-\tau^+_B/\delta_B)$.

However, not only one but several unbound phases may occur before $Protein_B$ is successfully synthesized. The number L of unbound phases until and including successful synthesis follows a geometric distribution, $P(L = l) = (1 - q)^{l-1}\, q$ with parameter $q = q_s \cdot q_t \cdot q_b$. The average number of unbound phases during a time interval Δt is $\tau^-_A \cdot \Delta t$. Thus, we can convert the random variable L into $T = L/\tau^-_A$ via a linear transformation of a random variable, giving the actual time until successful synthesis of $Protein_B$. Using the properties of the geometric distribution for the random variable T, we end up with the mean and the variance of the residence time:

$$t_s = \frac{1}{\tau^-_A \cdot q_s q_t q_b} \quad \text{and}$$
$$\sigma^2_{t_s} = \frac{1}{(\tau^-_A)^2} \cdot \frac{1 - q_s q_t q_b}{(q_s q_t q_b)^2}. \tag{13}$$

An important approximation for the residence time can be derived under the assumption of rapid translation and slow mRNA degradation, $\beta >> \gamma$, leading to $q_t \approx 1$. This implies that it is quite certain that an mRNA will be translated at least once before degradation. In the regime of rapid transcription factor binding ($\tau^+ >> \delta,\alpha$), the probability for a binding reaction is close to 1, $q_b \approx 1$, whereas the probability for at least one transcription can be approximated with $q_s \approx \alpha_B/(\tau_A^+ \overline{N}_A)$. Taken together, this leads to a linear dependence of the residence time on the protein number,

$$t_s \approx \left(\frac{\tau_A^+}{\tau_A^-}\right) \cdot \left(\frac{\overline{N}_A}{\alpha_B}\right). \quad (14)$$

We want to compare our analytical approximation with the residence time derived from simulations. To that end, we have to infer the dominating attractors from the simulated time courses. Recall that we can identify the dominating attractors via thresholds χ_A, χ_B at protein levels. The residence time of attractor S_A (S_B) is estimated as the consecutive time in a trajectory where $N_A > \chi_A$ ($N_B > \chi_B$). We compare the analytically derived geometric distribution for the residence times (see Eq. 13) with numerical results by simulating the switch with a given parameter set and estimating the residence times from 10,000 stochastic simulations. Fig. 4 *A* shows excellent agreement between the geometric distributed residence time and the simulations for a protein degradation rate of $\delta = 8 \cdot 10\ s^{-1}$. This legitimates the approximations and assumptions made above for the parameter regime of rapid transcription factor binding. From the analysis of the mean residence time for different protein half-lives, we find again a good agreement between the simulation and the approximation (see Fig. 4 *B*). Moreover, the slope of the log-log curve of the simulation is 1—confirming a linear dependence of the residence time from the mean protein level.

With the result from Eq. 13 we can compare the mean residence time of different switch models. To begin, we consider a gene expression model where transcription and translation are condensed into a single protein synthesis reaction. In analogy to the two-stage model of gene expression (26), this can be called a one-stage model of gene expression. To achieve the same amount of proteins at similar degradation rates, the synthesis rate in the one-stage model needs to be larger compared to the transcription and translation rates in the two-stage model. The probability q_t that accounts for translation during mRNA lifetime can be set to 1, because there is no mRNA stage and proteins are produced immediately. The binding probability q_b remains unchanged. However, because of the increased synthesis rate, the probability q_s of synthesis during the unbound phase will be larger than in the two-stage model. Therefore, the mean residence time will be decreased in the one-stage model as compared to the two-stage model, leading to more frequent attractor changes. This finding is in accordance with the previously reported stabilizing effect of bursts in an exclusive switch (16).

A second modification of the switch includes autoactivation of both genes. If the promoter of the gene is unbound it will be transcribed with a small basal rate κ. If the promoter is bound by its own protein product, the gene will be transcribed with full rate $\alpha >> \kappa$. Repressor-bound promoters are inactive. For simplicity, we assume that either activators or repressors are bound but not both at the same time. Note that, in this case, the deterministic ODE model is also bistable (42). Considering the mean residence time in a two-stage switch with autoactivation, we find that the probability q_s of mRNA synthesis during the unbound phase is smaller than in the ordinary two-stage model. Because no activator is present in this attractor, mRNA has to be transcribed with the small basal rate κ, making the transcription more improbable. The probability q_t for translation remains unchanged. However, the probability q_b of protein binding to the antagonistic promoter is also decreased because this promoter is occupied by the abundant activator most of the time. Therefore, repressor binding to this promoter requires an additional dissociation reaction of the activator during repressor

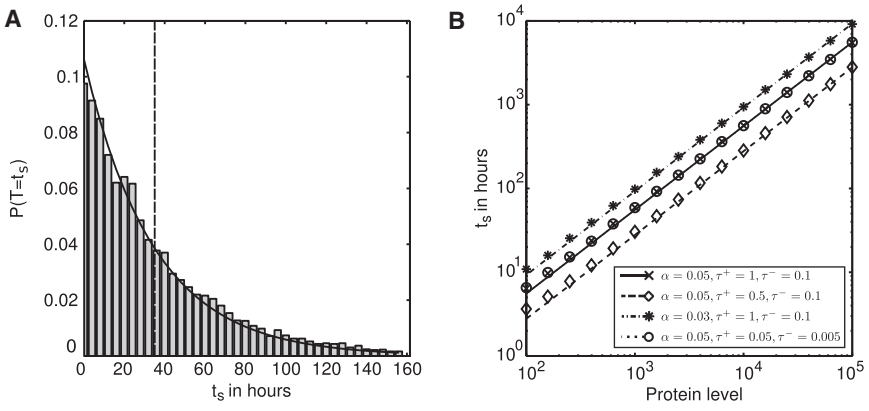

FIGURE 4 Residence time t_s in the two-stage toggle switch. (*A*) The distribution for t_s obtained by stochastic simulation is in good agreement with the geometric distribution derived from our mean-field approximation. (*Dashed line*) Mean of the distribution. The protein decay rate was set to $\delta = 8 \cdot 10^{-4}\ s^{-1}$. (*B*) Mean residence time t_s versus mean protein level $\overline{N}$ derived from stochastic simulation (*symbols*) and our analytical approximation (*lines*) for four different parameter settings. Note that the analytical approximations as well as the simulation results of the first and fourth parameter sets coincide. The exponent in the relation $t_s \propto (\overline{N}_A)^\nu$ is $\nu = 1$, in accordance with Eq. 4.

lifetime. As both q_s and q_b are decreased the mean residence time in switch models with autoactivation will be strongly increased compared to the ordinary two-stage model.

Summarizing, we find that the residence time is i), geometrically distributed; ii), the mean of the distribution grows linearly with the number of proteins for slow mRNA degradation; and iii), both the intermediate step of mRNA production and the autoactivation of transcription factors increase the residence time.

DISCUSSION

Lineage priming

We now discuss the implications of our findings in the context of cell differentiation driven by the toggle switch. In previous studies (8,9,40), attractors where either one or the other player is dominating, thereby repressing the antagonist (S_A, S_B), corresponded to committed cells. We also find analogs for the intermediate states S^*_A and S^*_B. In these attractors, the system has a strong preference toward one specific dominating attractor, but is not fully committed yet. A similar behavior is known as lineage priming in stem cell biology (43). Two different studies (44,45) showed that a population of stem and progenitor cells, respectively, can be divided into subpopulations that mainly give rise to only one of two possible cell types. In our simple model this would correspond to stem cells that reside either in S^*_A or S^*_B. These stem cells can still give rise to both cell fates but have a strong tendency toward one of them.

Remarkably, only a two-stage probabilistic model of the toggle switch shows dynamics reminiscent of lineage priming. Although a progenitor state exists in one-stage models of the toggle switch, cells in this state will move to either the one or the other committed state with equal probability.

Residence time

We find that the residence time in S_A and S_B, a key property of the system, is geometrically distributed. Previous contributions (22,23,46) focused only on the mean residence time and did not consider its underlying distribution. What does a geometric distribution for the residence time imply for the differentiation process dependent on the state of a genetic switch?

To discuss this question, let us first reason on how a differentiation decision could be established with the toggle switch lined out in the previous sections. We discriminate two scenarios for the differentiation of a cell:

In the first scenario, the state of the switch completely determines the cell fate. Starting in the progenitor attractors S^*_A or S^*_B, after a certain amount of time the switch will move to a committed attractor. We assume that the high numbers of proteins of the dominating player will trigger the differentiation program of the associated lineage and establish the mature cell type. However, due to stochasticity, the switch will drop out of the committed attractors and the cell will not only lose the current lineage decision, but possibly even switch to the opposing cell fate. To establish stable lineages in this scenario, the cell has to assure that the residence time of the switch is much longer than all relevant biological processes of the cell, especially cell lifetime. This guarantees that the cell will keep a lineage decision once it has obtained one. Yet the geometric distribution of the residence time imposes difficulties in this scenario: Even if the mean residence time is high, short residence times will always be more probable than longer residence times. The toggle switch could either be stabilized with the aforementioned autoactivation of the players, or with very high protein numbers so that the geometric distribution flattens and transforms to an almost uniform distribution. Both means would assure that only a very small percentage of a population of cells forgets its lineage decision during lifetime.

In the second scenario, we assume that the cell gets locked into one fate by changing the shape of the underlying potential so that further transitions between attractors become less possible. Such a change of the potential could, for example, be facilitated by chromatin changes, as proposed by Akashi et al. (47). In the following, we assume that only if one state dominates the other for a long enough fixation time t_d, downstream genes necessary for the decision process are activated (e.g., leading to chromatin remodeling), and the cell differentiates. Such a time-dependent property could be implemented with low-pass filters (see Narula et al. (48) for an example in hematopoietic stem cells) and would allow for an integration of external signals (see Rieger et al. (49) for the instructive power of hematopoietic cytokines). In this scenario, the residence time determines when differentiation will occur: The switch will constantly move into and out of the dominating attractors, until the residence time is finally long enough so that the dominating player can activate the downstream differentiation machinery. Ignoring the time the system spends in the intermediate attractors and just summing up the residence times in S_A and S_B until a long enough residence time for differentiation occurs, we find that this time follows a geometric-like distribution (see Section S5 in the Supporting Material). Under this differentiation mechanism, most cells will differentiate very fast and only a few cells will need longer. Experiments that measure the time for single cells needed to go from the primed to the committed state (as an extension to the two-day threshold reported by Heyworth et al. (50) for GM-CTC cells) to support or reject these hypotheses remain to be done.

Comparison to previous models

Finally, we discuss how our findings relate to previous studies on the toggle switch. We found that the mean of the residence time distribution scales linearly with the number of proteins in the system. The more proteins

present, the longer the average residence time in S_A or S_B. However, shorter residence times are still most probable due to the geometric distribution. This holds for the one-stage, the two-stage, and the autoactivating scenario.

This linear scaling differs from the exponential (23) or near-exponential (46) scaling described previously in the one-stage scenario. In contrast to our model, the model of Warren and ten Wolde (46) considers dimerization of the transcription factors, motivated by the fact that cooperative binding is necessary to achieve bistability in a deterministic framework (10). We showed that, as soon as stochastic fluctuations are introduced, a system with multiple attractors is achieved that can act as a proper switch with additional states of low coexpression. Including dimerization as a prerequisite for inhibition in a one-stage model will strongly increase the stability of the attractors $S_{A/B}$ (46). This is consistent with our findings: Instead of requiring translation of one protein of the suppressed species, we now require this rare event to happen twice during a short time-frame, which is much less probable. However, the inclusion of dimerization will have less effect on the two-stage switch: because proteins are typically synthesized in bursts (in our model, the average burst size is $\beta/\gamma = 10$) and dimerization is a fast process (46), as soon as one burst occurs almost certainly a dimer is formed and can inhibit the currently dominating player. Therefore, the probability of leaving the attractors $S_{A/B}$ is similar to a nondimeric inhibition.

Contrary to our results, Warren and ten Wolde (46) report that introduction of mRNAs reduces the stability of the switch. This discrepancy can be understood in the light of dimerization. In their one-stage model, dimerization is a key ingredient of stability, which is lost when introducing translational bursts (i.e., shot noise). As we considered monomeric transcription factor binding, stability does not rely on dimerization. Therefore, mRNAs increase the stability of the system, because they introduce additional conditions required for switching.

Due to these differences in the model, it is hard to resolve the discrepancy between our linear and the exponential scaling of residence time found by Bialek (23) and Warren and ten Wolde (46). However, we want to emphasize that the theoretical results shown in Warren and ten Wolde (46) only consider protein numbers up to 30. In this region our simulation results show slight deviations from the analytical linear dependence (Fig. 4). At such low protein numbers the system does not only leave the dominating attractor according to the mechanism described in our results. It is also likely that just due to fluctuations in the gene expression (not fluctuations in the promoter) the dominating attractor is left. This mechanism operates only at very small protein numbers and its probability rapidly decreases with rising protein numbers. Therefore, our results do not contradict the findings of Warren and ten Wolde (46), but actually consider a different parameter regime with higher protein numbers. Interestingly, the noise-driven attractor changes are also described by Kashiwagi et al. (51), where the authors link this mechanism to the selection of a favorable, less noisy attractor in *Escherichia coli* populations.

In another contribution, Morelli et al. (52) use the forward flux-sampling algorithm to assess the stability of a one-stage genetic toggle switch with dimeric transcription factor binding. They find a similar mechanism of attractor flipping that is based on the synthesis of the suppressed species due to promoter fluctuations. Using the forward flux sampling, they obtain estimates of the switching rate (the inverse of the mean residence time) for different amounts of fluctuations in DNA-protein interaction and dimerization. Morelli et al. (52) modulate the size of fluctuations at the promoter by varying the ratio of binding rate and synthesis rate, the adiabaticity parameter $\omega = \tau^+/\alpha$ (τ^- is adjusted to keep τ^+/τ^- constant). Small ω leads to strong fluctuations, whereas large ω reduces fluctuations. They find that increasing ω decreases the average switching rate and therefore stabilizes the switch. This dependency vanishes for $\omega > 5$, where the average switching rate remains constant. The latter is in accordance with our results in Eq. 14, where the mean residence time depends only on the ratio of τ^+ and τ^-, not on the absolute values and is therefore independent of ω. The dependency of the average switching rate for $\omega < 5$ is not predicted by Eqs. 3 and 4. It is also not visible in the stochastic simulations, where mean residence times of systems with $\omega = 1$ and $\omega = 20$ coincide (Fig. 4). The results of Morelli et al. (52) were simulated for an average number of proteins $\overline{N}_A = \overline{N}_B = 27$.

As mentioned above, in regions of very small protein numbers the system might leave the dominating attractor by a mechanism not captured by Eqs. 3 and 4, probably causing the difference of the results of Morelli et al. (52) and our results for small ω.

SUPPORTING MATERIAL

Five additional sections with supporting equations, five figures, and one table are available at http://www.biophysj.org/biophysj/supplemental/S0006-3495(11)05350-1.

We thank Jan Krumsiek, Robert Schlicht, Timm Schroeder, and Peter Swain for stimulating discussions and Christiane Dargatz and Dominik Wittmann for careful reading and thoughtful feedback on drafts of this manuscript. Thanks to Sabine Hug and Daniel Schmidl for their help concerning the stability analysis. Moreover, we acknowledge the comments of the unknown reviewers, who improved the quality of the manuscript.

This work was supported by the Helmholtz Alliance on Systems Biology (project "CoReNe"), the European Research Council (starting grant "LatentCauses"), and the German Science Foundation DFG (postdoctoral fellowship MA 5282/1-1 for C.M. and SPP 1356 "Pluripotency and Cellular Reprogramming").

REFERENCES

1. Orkin, S. H., and L. I. Zon. 2008. SnapShot: hematopoiesis. *Cell.* 132:712.

2. Krumsiek, J., C. Marr, …, F. J. Theis. 2011. Hierarchical differentiation of myeloid progenitors is encoded in the transcription factor network. *PLoS ONE.* 6:e22649.
3. Zhang, P., G. Behre, …, Z. Sun. 1999. Negative cross-talk between hematopoietic regulators: GATA proteins repress PU.1. *Proc. Natl. Acad. Sci. USA.* 96:8705–8710.
4. Arinobu, Y., S.-i. Mizuno, …, K. Akashi. 2007. Reciprocal activation of GATA-1 and PU.1 marks initial specification of hematopoietic stem cells into myeloerythroid and myelolymphoid lineages. *Cell Stem Cell.* 1:416–427.
5. Burda, P., P. Laslo, and T. Stopka. 2010. The role of PU.1 and GATA-1 transcription factors during normal and leukemogenic hematopoiesis. *Leukemia.* 24:1249–1257.
6. Macarthur, B. D., A. Ma'ayan, and I. R. Lemischka. 2009. Systems biology of stem cell fate and cellular reprogramming. *Nat. Rev. Mol. Cell Biol.* 10:672–681.
7. Cherry, J. L., and F. R. Adler. 2000. How to make a biological switch. *J. Theor. Biol.* 203:117–133.
8. Roeder, I., and I. Glauche. 2006. Towards an understanding of lineage specification in hematopoietic stem cells: a mathematical model for the interaction of transcription factors GATA-1 and PU.1. *J. Theor. Biol.* 241:852–865.
9. Huang, S., Y.-P. Guo, …, T. Enver. 2007. Bifurcation dynamics in lineage-commitment in bipotent progenitor cells. *Dev. Biol.* 305: 695–713.
10. Chickarmane, V., T. Enver, and C. Peterson. 2009. Computational modeling of the hematopoietic erythroid-myeloid switch reveals insights into cooperativity, priming, and irreversibility. *PLOS Comput. Biol.* 5:e1000268.
11. Duff, C., K. Smith-Miles, …, T. Tian. 2011. Mathematical modeling of stem cell differentiation: the PU.1-GATA-1 interaction. *J. Math. Biol.* 2011 Apr 2. [Epub ahead of print].
12. Eldar, A., and M. B. Elowitz. 2010. Functional roles for noise in genetic circuits. *Nature.* 467:167–173.
13. Paulsson, J. 2005. Models of stochastic gene expression. *Phys. Life Rev.* 2:157–175.
14. Kepler, T. B., and T. C. Elston. 2001. Stochasticity in transcriptional regulation: origins, consequences, and mathematical representations. *Biophys. J.* 81:3116–3136.
15. Warren, P. B., and P. R. ten Wolde. 2004. Enhancement of the stability of genetic switches by overlapping upstream regulatory domains. *Phys. Rev. Lett.* 92:128101.
16. Schultz, D., A. M. Walczak, …, P. G. Wolynes. 2008. Extinction and resurrection in gene networks. *Proc. Natl. Acad. Sci. USA.* 105:19165–19170.
17. Walczak, A. M., J. N. Onuchic, and P. G. Wolynes. 2005. Absolute rate theories of epigenetic stability. *Proc. Natl. Acad. Sci. USA.* 102:18926–18931.
18. Lipshtat, A., A. Loinger, …, O. Biham. 2006. Genetic toggle switch without cooperative binding. *Phys. Rev. Lett.* 96:188101.
19. Walczak, A. M., M. Sasai, and P. G. Wolynes. 2005. Self-consistent proteomic field theory of stochastic gene switches. *Biophys. J.* 88:828–850.
20. Schultz, D., J. N. Onuchic, and P. G. Wolynes. 2007. Understanding stochastic simulations of the smallest genetic networks. *J. Chem. Phys.* 126:245102.
21. Loinger, A., A. Lipshtat, …, O. Biham. 2007. Stochastic simulations of genetic switch systems. *Phys. Rev. E Stat. Nonlin. Soft Matter Phys.* 75:021904.
22. Barzel, B., and O. Biham. 2008. Calculation of switching times in the genetic toggle switch and other bistable systems. *Phys. Rev. E Stat. Nonlin. Soft Matter Phys.* 78:041919.
23. Bialek, W. 2001. Stability and noise in biochemical switches. *In* Advances in Neural Information Processing Systems 13..; The MIT Press, Cambridge, MA. 103.
24. Zhu, R., A. S. Ribeiro, …, S. A. Kauffman. 2007. Studying genetic regulatory networks at the molecular level: delayed reaction stochastic models. *J. Theor. Biol.* 246:725–745.
25. Thattai, M., and A. van Oudenaarden. 2001. Intrinsic noise in gene regulatory networks. *Proc. Natl. Acad. Sci. USA.* 98:8614–8619.
26. Shahrezaei, V., and P. S. Swain. 2008. Analytical distributions for stochastic gene expression. *Proc. Natl. Acad. Sci. USA.* 105:17256–17261.
27. Warren, L., D. Bryder, …, S. R. Quake. 2006. Transcription factor profiling in individual hematopoietic progenitors by digital RT-PCR. *Proc. Natl. Acad. Sci. USA.* 103:17807–17812.
28. Gardner, T. S., C. R. Cantor, and J. J. Collins. 2000. Construction of a genetic toggle switch in *Escherichia coli*. *Nature.* 403:339–342.
29. Reference deleted in proof.
30. Harper, C. V., B. Finkenstädt, …, M. R. White. 2011. Dynamic analysis of stochastic transcription cycles. *PLoS Biol.* 9:e1000607.
31. Raj, A., C. S. Peskin, …, S. Tyagi. 2006. Stochastic mRNA synthesis in mammalian cells. *PLoS Biol.* 4:e309.
32. Müller-Herold, U. 1975. General mass-action kinetics. Positiveness of concentrations as structural property of Horn's equation. *Chem. Phys. Lett.* 33:467–470.
33. Van Kampen, N. G. 1992. Stochastic Processes in Physics and Chemistry. North-Holland, Amsterdam, The Netherlands.
34. Gillespie, D. T. 2007. Stochastic simulation of chemical kinetics. *Annu. Rev. Phys. Chem.* 58:35–55.
35. Taniguchi, Y., P. J. Choi, …, X. S. Xie. 2010. Quantifying *E. coli* proteome and transcriptome with single-molecule sensitivity in single cells. *Science.* 329:533–538.
36. Walczak, A., A. Mugler, and C. Wiggins. 2010. Analytic methods for modeling stochastic regulatory networks. Arxiv preprint arXiv: 1005.2648.
37. Gillespie, D. 1977. Exact stochastic simulation of coupled chemical reactions. *J. Phys. Chem.* 81:2340–2361.
38. Li, H., Y. Cao, …, D. T. Gillespie. 2008. Algorithms and software for stochastic simulation of biochemical reacting systems. *Biotechnol. Prog.* 24:56–61.
39. Wang, J., L. Xu, and E. Wang. 2008. Potential landscape and flux framework of nonequilibrium networks: robustness, dissipation, and coherence of biochemical oscillations. *Proc. Natl. Acad. Sci. USA.* 105:12271–12276.
40. Wang, J., L. Xu, …, S. Huang. 2010. The potential landscape of genetic circuits imposes the arrow of time in stem cell differentiation. *Biophys. J.* 99:29–39.
41. Waddington, C. H. 1957. The Strategy of the Genes: A Discussion of Some Aspects of Theoretical Biology. George Allen & Unwin, London, UK.
42. Siegal-Gaskins, D., M. K. Mejia-Guerra, …, E. Grotewold. 2011. Emergence of switch-like behavior in a large family of simple biochemical networks. *PLOS Comput. Biol.* 7:e1002039.
43. Graf, T., and M. Stadtfeld. 2008. Heterogeneity of embryonic and adult stem cells. *Cell Stem Cell.* 3:480–483.
44. Müller-Sieburg, C. E., R. H. Cho, …, H. B. Sieburg. 2002. Deterministic regulation of hematopoietic stem cell self-renewal and differentiation. *Blood.* 100:1302–1309.
45. Chang, H. H., M. Hemberg, …, S. Huang. 2008. Transcriptome-wide noise controls lineage choice in mammalian progenitor cells. *Nature.* 453:544–547.
46. Warren, P. B., and P. R. ten Wolde. 2005. Chemical models of genetic toggle switches. *J. Phys. Chem. B.* 109:6812–6823.
47. Akashi, K., X. He, …, L. Li. 2003. Transcriptional accessibility for genes of multiple tissues and hematopoietic lineages is hierarchically controlled during early hematopoiesis. *Blood.* 101:383–389.
48. Narula, J., A. M. Smith, …, O. A. Igoshin. 2010. Modeling reveals bistability and low-pass filtering in the network module determining blood stem cell fate. *PLOS Comput. Biol.* 6:e1000771.

49. Rieger, M. A., P. S. Hoppe, …, T. Schroeder. 2009. Hematopoietic cytokines can instruct lineage choice. *Science.* 325:217–218.

50. Heyworth, C., S. Pearson, …, T. Enver. 2002. Transcription factor-mediated lineage switching reveals plasticity in primary committed progenitor cells. *EMBO J.* 21:3770–3781.

51. Kashiwagi, A., I. Urabe, …, T. Yomo. 2006. Adaptive response of a gene network to environmental changes by fitness-induced attractor selection. *PLoS ONE.* 1:e49.

52. Morelli, M. J., S. Tanase-Nicola, …, P. R. ten Wolde. 2008. Reaction coordinates for the flipping of genetic switches. *Biophys. J.* 94:3413–3423.